ELSEVIER

Polymer 42 (2001) 7791–7799

polymer

www.elsevier.nl/locate/polymer

Hygrothermal diffusion behavior in bismaleimide resin

Yanmei Li, John Miranda, Hung-Jue Sue*

Department of Mechanical Engineering, Polymer Technology Center, Texas A & M University, College Station, TX 77843-3123, USA

Received 18 December 2000; received in revised form 22 March 2001; accepted 24 March 2001

Abstract

Hygrothermal diffusion behavior of bismaleimide resin prepared by two different curing schedules is studied. The Langmuir model is employed to describe the non-Fickian diffusion behavior observed at two different hygrothermal conditioning temperatures. Dynamic mechanical analysis, attenuated-total-reflectance Fourier transform infrared spectroscopy and swelling experiments were conducted to investigate the nature of the diffusion process. The experimental findings reveal that both hydrogen bonding and the nature of the network architecture strongly affect the hygrothermal diffusion behavior of the bismaleimide resin. The possible diffusion mechanisms accounted for such a non-Fickian diffusion behavior are discussed.

Keywords: Bismaleimide resin; Hygrothermal behavior; Moisture diffusion

1. Introduction

Thermoset bismaleimide (BMI) resins have evolved as important matrix materials for polymer composites because of their 'epoxy-like' processing characteristics, superior thermal stability and fatigue resistance at high humidity [1–3]. A major drawback of BMI resins is their brittleness, which is attributed to the high crosslinking density nature of the cured network [4]. In recent years, many BMI resins have been modified to improve their toughness [5]. The BMI resin used in this study is a three-component toughened BMI resin [6], which has a trade name of Cytec 5250-4-RTM BMI.

It is well recognized that BMI is considered as a matrix for high-temperature aerospace structural applications and expected to experience extreme environmental conditions for a prolonged period of time. Environmental aging in polymer composites, particularly for that caused by hygrothermal aging, is of interest to many applications. Since the fiber is carbon and absorbs a negligible amount of moisture, if any, it is natural that we focus on studying the fundamental moisture diffusion behavior of neat polymer matrices for long-term composite performance [7]. The effects of hygrothermal conditioning on BMI resins and their composites were studied by many researchers [7–11]. Various conclusions have been drawn about the moisture absorption behavior in BMI [7,8,10,11]. Change in material properties such as glass transition temperature [8–10] and density [10] due to hygrothermal conditioning have also been reported. Both Fickian [8] and non-Fickian diffusion [7,10,11] behaviors have been observed in BMI resins.

Extensive work has been performed focusing on moisture absorption mechanisms in epoxy-resin [12–18], but not in BMI resins. The objective of this study is to investigate the diffusion mechanisms and diffusion behavior in BMI resins. Apicella et al. [16] propose that there may be three ways for epoxy resins to absorb water: (1) formation of polymer-diluent solution; (2) adsorption at hydrophilic sites; (3) adsorption on the surface of free volume elements. Adamson [17] postulates that the transport of moisture below T_g is a three-stage process. First, water occupies the free volume in the form of voids. Water then becomes bound to network sites, causing swelling. Finally, it enters the densely crosslinked regions. Carter and Kibler [18] suggest that the spatial distribution of unbound water molecules becomes essentially uniform across the dimensions of a thin specimen long before the specimen is saturated with bound water molecules.

Both the polarity and topology of the network structure of epoxy resins are found to affect the absorption behavior [14,15]. Considering the interaction between water and polar groups in thermoset polymers, the widely used Fick's law is less appealing here since its assumption doesn't involve this interaction, which may be the main source of the observed non-Fickian diffusion behavior. Non-Fickian diffusion behavior was observed in the same BMI resin previously [7,11]. The main objective of this study is to

* Corresponding author. Tel: +1-979-845-5024; fax: +1-979-845-3081.
E-mail address: hjsu@acs.tamu.edu (H.-J. Sue).

0032-3861/01/$ - see front matter
PII: S0032-3861(01)00241-5

investigate mechanisms that are responsible for this non-Fickian diffusion process.

Two well-accepted models, which were proposed to account for the interaction between water and polymers, are the dual-mode sorption model [19–26] and the Langmuir model [18]. The essence of these two models is the hypothesis of the existence of mobile/immobile or bound/unbound water types in the system. The dual-mode sorption model [19–21] is normally used to describe the solution and diffusion of gases in glassy polymers, and the permeation of gases through glassy polymer membranes. In this model, it is assumed that gas molecules either are sorbed by an ordinary dissolution mechanism that obeys the Henry's law [19,20], or reside in pre-existing 'holes' described by the Langmuir isotherm [19,20]. Earlier studies assumed that the population dissolved by ordinary dissolution in the Henry's law domains was totally mobile, whereas the population dissolved in the Langmuir domains was totally immobilized. This assumption was later relaxed by Paul and Koros [22,23] and by Petropoulos [24], who modified the dual-mode sorption model, to better match the experimental results. The original dual-mode sorption model assumed that the plasticization effects could be neglected since the penetrant's solubility in the polymer was very low. However, such effects are known to be operative in many important practical applications. Therefore, Stern et al. [25,26] extended the dual-mode sorption model to take into account the effects of plasiticization.

The Langmuir model proposed by Carter and Kibler [18] has been employed successfully in many practical studies [27–29] to describe the non-Fickian diffusion in polymers. In the Langmuir model [18], it is assumed that diffusivity, D_γ, is both concentration- and stress-independent. Water is assumed to be absorbed, and has a probability per unit time, γ, of becoming bound. Water molecules that are emitted from the bound phase, which become unbound, are assumed to be departing with a probability per unit time β. An equilibrium moisture uptake, M_∞, is obtained when the number of mobile molecules per unit volume, n, and the number of bound molecules per unit volume, N, approach values such that $\gamma n = \beta N$. A useful approximation for the total moisture uptake is:

$$M_t \cong M_\infty \left\{ \frac{\beta}{\gamma+\beta} e^{-\gamma t} \left[1 - \frac{8}{\pi^2} \sum_{l=1}^{\infty\,(\text{odd})} \frac{e^{-\kappa l^2 t}}{l^2} \right] + \frac{\beta}{\gamma+\beta}(e^{-\beta t} - e^{-\gamma t}) + (1 - e^{-\beta t}) \right\}, \quad (1)$$

$$2\gamma, 2\beta \leq \kappa$$

where M_t is the moisture uptake percentage at time t, l the specimen thickness, and $\kappa = \pi^2 D_\gamma / l^2$. The BMI resin used in this study has polar groups such as hydroxyl groups. The hydroxyl group can form hydrogen bonds with water during the diffusion process. Hydrogen-bonded water can be considered bound water. It has a specific probability of becoming unbound water. In contrast to the dual-mode model, the Lang muir model has fewer fitting parameters and is derived based on similar physical grounds. Therefore, the Langmuir model is chosen in this study to describe this diffusion process.

The change of topology of molecular structure is expected to affect the diffusion process. Thus, two curing schedules were used to prepare two BMIs with two different network structures. The hygrothermal conditioning temperature plays an important role in altering hydrogen bonding nature during the diffusion process. Two hygrothermal conditioning temperatures at 70 and 100°C were chosen for the present study. The boiling temperature for water is 100°C at 1 atm. The chance for water to form hydrogen bond at this temperature is reduced. Hence, 70 and 100°C were chosen to take into account temperature effects on the formation of bound/unbound water. It is expected that the variations in molecular topology and conditioning temperature can help reveal the fundamental knowledge pertaining the non-Fickian diffusion behavior in BMI.

2. Experimental procedure

2.1. Material

The Cytec 5250-4-RTM BMI resin used in this study is a three-component BMI. It consists of 4,4′-bismaleimidiphenylmethane (BMPM), *O*,*O*′-diallyl bisphenol A (DABPA) and BMI-1,3-tolyl. The BMI panels were prepared using an infusion molding process at 190°C for 6 h and then at two postcuring temperatures of 218 and 230°C, respectively, for another 6 h. The 230°C postcuring is the recommended postcuring temperature by the manufacturer. No observable microcracks were found in the bulk resin upon cooling even after careful optical microscopy examinations. The panel postcured at 218°C was labeled as L-BMI, and the one postcured at 230°C was labeled as H-BMI.

2.2. Moisture absorption experiment

Specimens with dimensions of $25 \times 25 \times 2\ \text{mm}^3$ (length × width × thickness) were cut from the laminates with a diamond saw. Specimens were dried in a vacuum oven at 80°C under a vacuum of 30 in.Hg until a constant weight was achieved. They were then put into a humidity chamber and exposed to 100% relative humidity (RH) air and constant temperatures of 70 and 100°C, respectively. Specimens were taken out of the chamber and weighed periodically using an analytical balance having a precision of ±0.0001 g. The specimen weighing time interval was set about two hours during the first day of moisture conditioning experiment. After that, specimens were weighed daily during the first week of conditioning. Specimens were then weighed weekly until the end of the study. The measurement time was subtracted from the calculated exposure

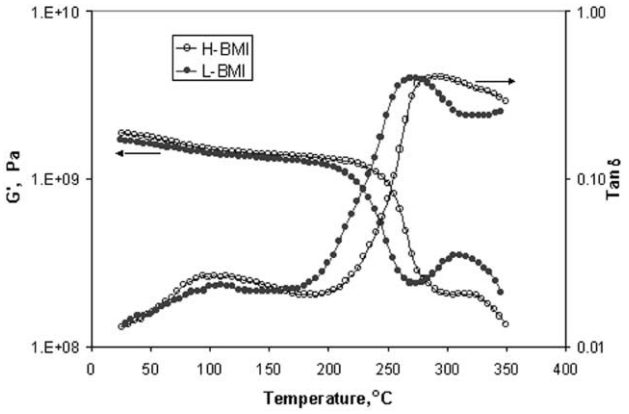

Fig. 1. DMA spectra of BMI prepared at two different posturing temperatures.

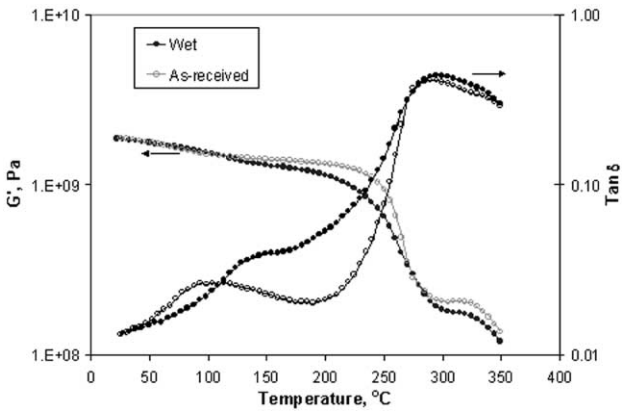

Fig. 3. DMA spectra of H-BMI with and without hygrothermal conditioning at 70°C and 100% RH.

time. Weight gain of the specimen, M, was calculated by the following equation: $M = [(W - W_d)/W_d] \times 100\%$, where W_d is the weight of the dried specimen and W the weight of the specimen at a given exposure time. The weight gain, M, vs. the square root of exposure time over thickness was plotted to generate moisture absorption curves. At least three specimens were used for each type of BMI in the absorption experiments. The average values were reported.

2.3. Dynamic mechanical analysis

Dynamic mechanical analysis (Rheometrics RMS-800) was performed on BMI resin in a torsion mode, with 5°C per step. A 0.1% sinusoidal strain and a frequency of 1 Hz were used. The samples were tested at temperatures ranging from 25 to 380°C. The temperature at which the maximum tan δ value is located is assigned as glass transition temperatures (T_g).

2.4. ATR-FTIR spectroscopy

Attenuated-total-reflectance Fourier transform infrared (ATR-FTIR) spectroscopy analysis was performed on sample surfaces using a Nicolet AVATAR 360 system with a resolution of 2 cm^{-1}. The scanned wave-number range was 4000–700 cm^{-1}. For moisture conditioned samples, ATR-FTIR was performed at room temperature immediately after the samples were taken out of the humidity chamber.

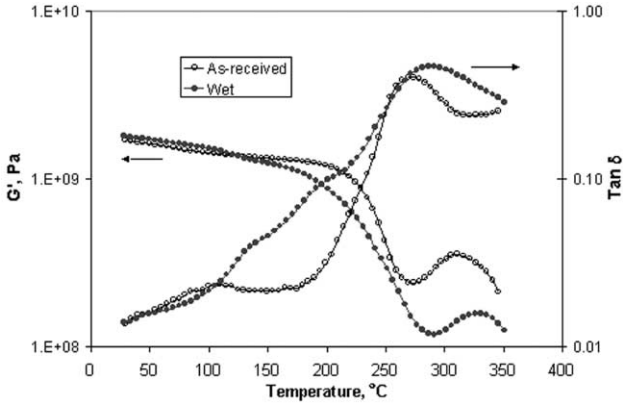

Fig. 2. DMA spectra of L-BMI with and without hygrothermal conditioning at 70°C and 100% RH.

2.5. Swelling experiment

Since the dimensional change is too small to be measured by a caliper, the dimensional changes of the specimens were quantified by the liquid displacement method. Testing was conducted on the conditioned specimens with different moisture uptakes. Apparent volume V (volume of polymer and moisture) was calculated using: $V = M/\rho$, where M is the mass and ρ the density of the specimen. Density was determined according to the ASTM standard D792. Then, the volume change was calculated using: $\Delta V = [(V - V_0)/V_0] \times 100\%$, V_0 is the volume of dried sample before the absorption test. At least three specimens were used in this experiment.

3. Results

3.1. DMA spectra of BMIs

DMA was used to probe the molecular structure of materials prepared at two postcuring temperatures. As shown in Fig. 1, the postcuring temperature has a great effect on the DMA spectra of BMI. Shear storage modulus, G', of L-BMI starts to drop dramatically at temperatures lower than that of H-BMI. The increase in G' right after T_g in L-BMI indicates further curing of BMI during the DMA testing. One should note that the decrease in G' of both BMIs above 320°C is most likely due to the degradation of the specimens. The T_g of L-BMI and H-BMI are 270 and 290°C, respectively. H-BMI is believed to have a higher crosslinking density because of its higher T_g.

In Figs. 2–4, wet sample indicates that the sample

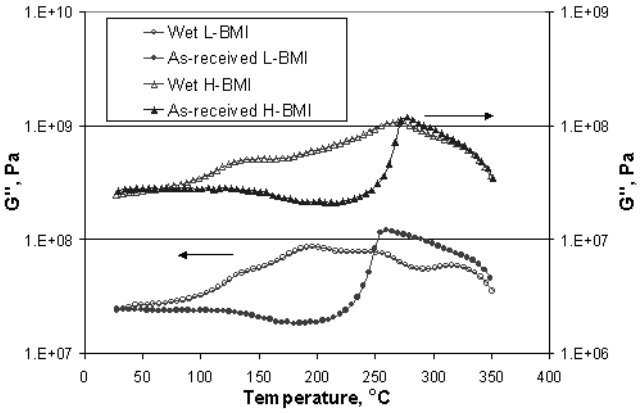

Fig. 4. G'' spectra of BMI with and without hygrothermal conditioning at 70°C and 100% RH.

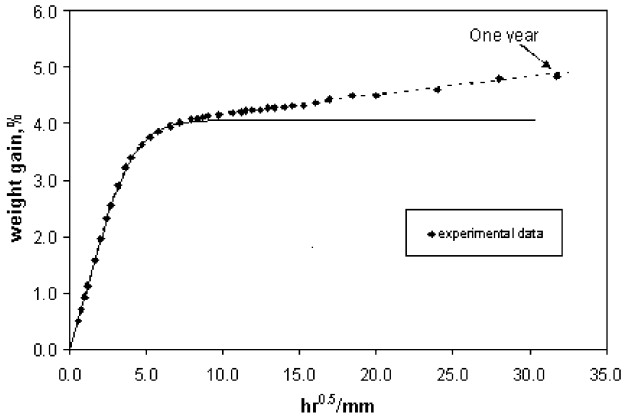

Fig. 6. Moisture diffusion in L-BMI at 70°C and 100% RH. (The solid line is a Fickian fit, and the dashed line is based on a Langmuir fit.)

contains 4.5% moisture uptake and was conditioned at 70°C and 100% RH. It can be seen that G' of both wet BMIs starts to decrease at around 120°C due to the plasticization caused by the absorbed moisture. The plasticization effect is more significant in L-BMI. The T_g values of H-BMI before and after conditioning are almost the same, while the T_g of L-BMI is increased by about 20°C after hygrothermal conditioning. Caution should be taken in interpreting the DMA results of L-BMI. Firstly, L-BMI is not fully cured. Further curing is possible at the temperature close to T_g during the DMA testing. Secondly, water has a great effect on the DMA spectra of L-BMI, and this effect is not well understood. As shown in Fig. 4, there is no obvious G' peak around the α-transition temperature for wet L-BMI.

3.2. Moisture absorption in BMI

Fig. 5 is the weight change profile for two BMI resins under two different hygrothermal conditioning temperatures at 100% RH. It is apparent that both BMI resins have similar diffusion behaviors. The experimental data match the Fickian curves well during the initial stage of moisture absorption, but diverge from the Fick's equilibrium moisture uptake, M_f, with time (Fig. 6). This behavior was also observed by others [30]. The Fickian curve (solid line) was plotted according to a simplified solution [31] to the Fick's second law:

$$\frac{M_t}{M_f} = 1 - \exp\left[-7.3\left(\frac{Dt}{l^2}\right)^{3/4}\right] \quad (2)$$

where M_t is the water percentage at time t and l the specimen thickness. Diffusivity (D) and Fickian equilibrium moisture uptake, M_f, were determined by fitting experimental data into Eq. (2). The Langmuir curve (dashed line) is plotted according to Eq. (1). D_γ is the same as D determined from Fickian fitting (Eq. (2)). The parameters β, γ, and M_∞ are determined by fitting long-term experimental data into Eq. (1). As seen in Fig. 6, the Langmuir curve fits the entire range of the experimental data well. This suggests that the bound and unbound water concept can be used to describe the non-Fickian behavior in BMI. This hypothesis is further supported by the results of FTIR and the swelling experiment to be discussed below.

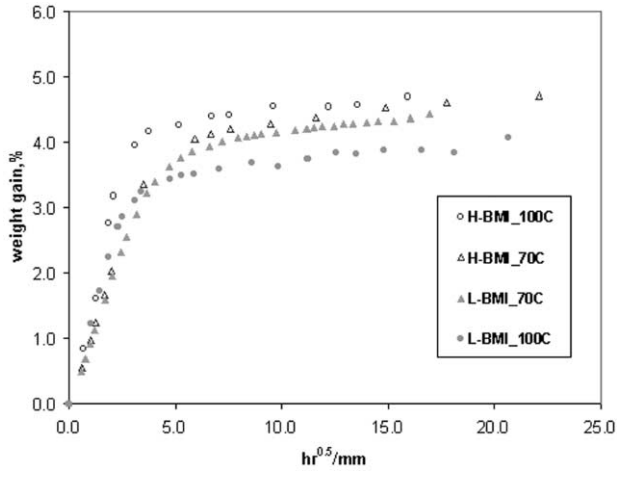

Fig. 5. Moisture absorption curves of two BMIs at two different hygrothermal conditioning temperatures and 100% RH.

Table 1 is the summary of D and M_f obtained from Fickian fits of the two BMIs. At two different hygrothermal conditioning temperatures, M_f and D of H-BMI are all higher than those of L-BMI. The above differences can be rationalized based on the free volume concept [14,32]. H-BMI has higher crosslinking density, thus containing higher frozen-in free volume formed during cooling from

Table 1
Summary of the moisture absorption study

Specimen	Diffusivity (10^{-6} mm^2/s)		M_f[a] (wt%)	
	70°C	100°C	70°C	100°C
L-BMI	2.58	6.00	4.06	3.50
H-BMI	2.80	6.50	4.20	4.35

[a] Moisture uptake at assumed Fickian plateau.

Table 2
Fitting parameters for the Langmuir model

Temperature (°C)	Specimen	β (10^{-4} h^{-1}	γ (10^{-4} h^{-1})	M_∞ (%)
70	L-BMI	2.0	0.5	5.2
	H-BMI	7.0	2.0	5.3
100	L-BMI	20	4.0	4.2
	H-BMI	30	4.0	4.8

the postcuring temperature [14]. Higher free volume results in higher D and M_f.

Table 2 is the summary of fitting parameters for Langmuir model. It is clearly shown that the probability for water to become unbound, β, is greater than that at lower temperatures for both BMIs. Although γ also increases with temperature, it is much smaller than β. Therefore the increase in β is more significant than the increase in γ. It should be noted that M_∞ values in the Langmuir model are all higher than those of M_f, since M_∞ accounts for two types of water as proposed in Langmuir model:

$$\text{Absorbed water} = \text{bound water} + \text{unbound water} \quad (3)$$

The trend in M_∞ with increasing temperature in two BMIs is the same, i.e. M_∞ decreases as temperature increases. If comparison is made using M_f, the trend turns out to be reversed in two BMIs, i.e. M_f of 100°C is lower than that of 70°C in L-BMI resin, while the opposite is found in H-BMI resin. As discussed above, it is more reasonable to compare M_∞ instead of M_f.

3.3. FTIR results

The three-component BMI used in this study consists of BMPM, DABPA and BMI-1,3-tolyl. Since the third component, BMI-1,3-tolyl, has a similar chemical structure of BMPM, the curing mechanisms of the three-component BMI are similar to that of the two-component BMI, which consists of BMPM and DABPA. The chemical reactions between BMPM and DABPA were thoroughly investigated by many researchers [33–37]. It has been found that BMPM and DABPA monomers react via the 'ene' reaction at low curing temperatures. The 'ene' adduct is penta-functional as a result of three double –C=C– bonds, capable of chain extension and crosslinking, and two hydroxyl groups, capable of etherification by hydroxyl dehydration. Other reaction types, such as Diels–Alder, homopolymerization, rearomatization, and alternating copolymerization, were also proposed to take place at different curing temperatures. In this study, two BMIs were cured at 190°C for 6 h, then postcured at two different temperatures, i.e. 218 and 230°C, respectively, for another 6 h. The network structure is therefore mainly affected by the postcuring stage.

Chemical compositions of two BMIs were characterized using the ATR-FTIR technique (Fig. 7). It is found that they have almost identical spectra. The FTIR peaks at 825, 919 and 1150 cm^{-1} are assigned to the maleimide C=C, allyl=CH_2 and maleimide C–N–C groups, respectively, in the prepolymer. The peaks at 919 and 1150 cm^{-1} will disappear after curing, and a new peak at 1181 cm^{-1}, which corresponds to succinimide C–N–C, is observed after curing. The peaks at 825 cm^{-1} for the two BMIs indicate the unconverted maleimide group. Their peak intensities are found inversely proportional to the degree of crosslinking. Since the principal cure reactions involve –C=C– double bonds, it is reasonable to assume that the two BMIs exhibit similar hydrophilicity. However, it is unclear how the unconverted reactants affect the diffusion behavior of BMI at the present time. From FTIR results, it is found that no new peak appears and no existing peaks disappear after hygrothermal conditioning. This suggests that no obvious chemical reaction, such as hydrolysis, has taken place due to the hygrothermal conditioning. Further study shows that the effect of water on the spectra of two BMIs is the same.

Infrared spectra obtained for moisture absorption as a

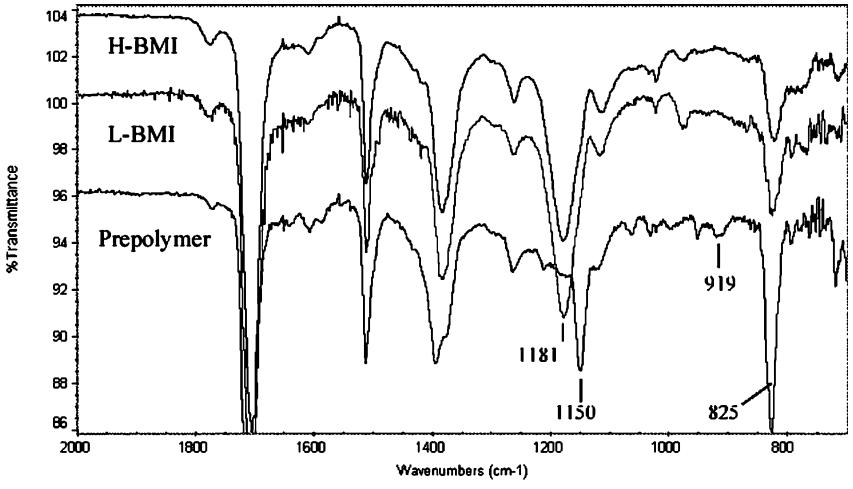

Fig. 7. FTIR of two BMIs prepared at two different curing schedules.

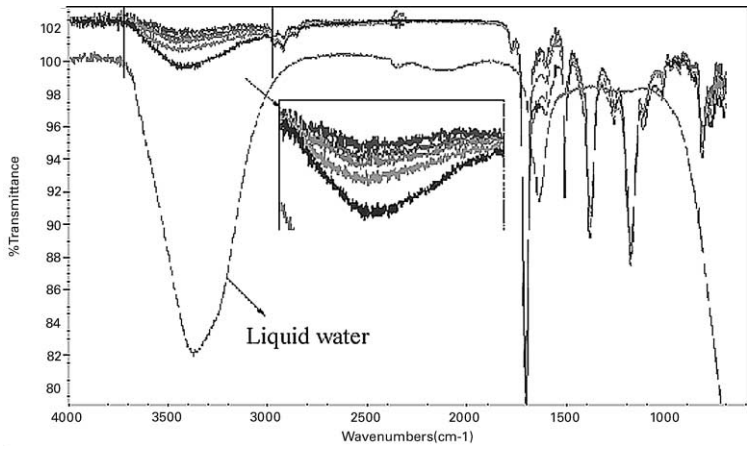

Fig. 8. FTIR spectrum of H-BMI condtioned at 70°C and 100% RH. (The curves in the zoom-in frame from top to bottom represent the samples hygrothermally conditioned at 0, 1, 12 h, 7 days, 3 months.)

function of time at 70°C are shown in Fig. 8. Comparison with pure liquid water is made as a reference in the same plot. For the spectrum of water, broad peaks between 3000 and 3700 cm^{-1} and a peak at 1638 cm^{-1} are assigned to the υ(OH) stretching and δ(OH) bending, respectively. Since BMI has –OH functional group, it also shows a broad peak in the 3000–3700 cm^{-1} region. As shown in the zoom-in frame, the broad peak in the 3000–3700 cm^{-1} in H-BMI is shifted to a lower frequency toward the position of υ(OH) in pure water, and the peak intensity increases as the amount of water in BMI increases. In the meantime, the shoulder intensity of the peak at 1607 cm^{-1}, which corresponds to the δ(OH) in the water, also increases with moisture uptake. The observations made on BMI hygrothermally conditioned at 100°C and 100% RH are similar to the above findings.

It is noted that the FTIR peak corresponding to free water absorption (at 3615 cm^{-1}) is hardly detectable. As a result, the level of hydrogen bonding formed in BMI can be quantified by the peak intensity in the region of 3000–3700 cm^{-1}.

The peak shifting at 3000–3700 cm^{-1} is observed in hygrothermally conditioned BMI. This suggests that hydrogen bonding has taken place between water and the polymer matrix [38–40]. Since the aromatic carbon–carbon stretching vibration at 1512 cm^{-1} is unaffected by the hygrothermal conditioning, this peak can be used as an internal reference peak to normalize OH stretching peak intensity:

$$\text{Peak intenstiy ratio} = \frac{\text{Peak intensity of OH stretching}}{\text{Peak intensity of aromatic C–C stretching}} \quad (4)$$

As shown in Fig. 9, peak intensity ratios for both temperatures increase gradually below 3.5% moisture uptake, but greatly increase at higher moisture contents. As will be discussed in the swelling experimental findings, the formation of hydrogen bonds dominates the later stages of the diffusion process, and this accounts for the non-Fickian behavior. Note that the peak intensity ratio for the 100°C conditioned sample increases at lower magnitudes, which is expected as the formation of hydrogen bonds is hindered by adding heat:

$$\text{Unbound water} + \text{Polar group} \rightarrow \text{Bound water} + \text{Heat} \quad (5)$$

3.4. Swelling test

Since the water molecule is polar in nature, it is capable of forming hydrogen bonds with the polar groups in BMI resin, thereby disrupting intra-chain hydrogen bonding between polar groups in the network. The net effect of this is an increase in the inter-segmental hydrogen bond length [41,42], which is called swelling. Adamson [17] proposed that bound water molecules, which cause most of the swelling, are immobilized by the polar groups in the polymer matrix; the unbound water molecules, which cause little or no swelling, are contained in the polymer free volume.

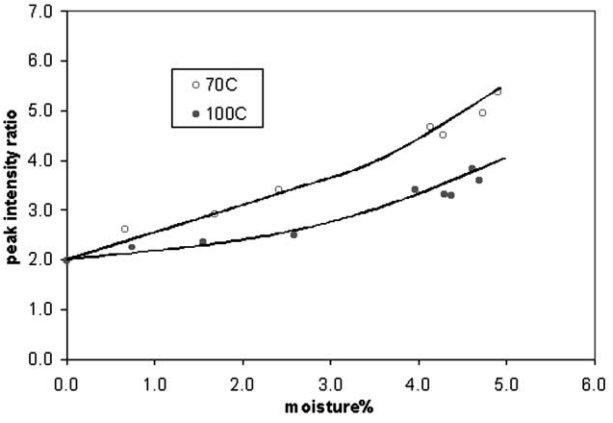

Fig. 9. Changes in peak intensity ratio (3000–3700 cm^{-1}) as a function of moisture content for H-BMI at two different temperatures.

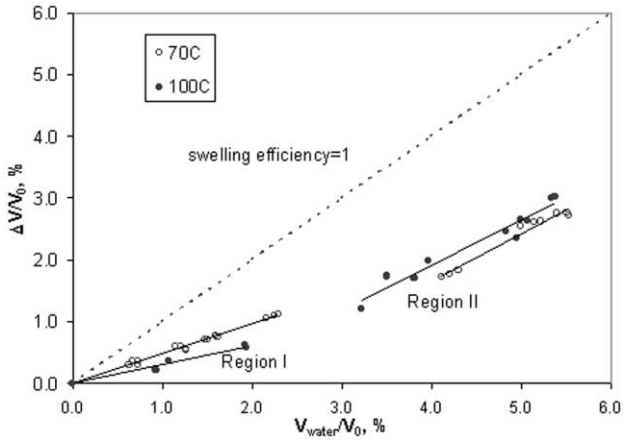

Fig. 10. Volume change of H-BMI during absorption at two different temperatures.

It may take several years for moisture absorption to reach saturation, depending on the nature of the polymer matrix.

Fig. 10 shows the percentage change in resin volume during hygrothermal conditioning normalized by the volume of dry resin, V_0, as a function of the net volume of absorbed water calculated from the change in specimen weight (also normalized by V_0). A dashed line having a slope of 1 represents swelling that would be expected if the volumes of the dry resin and the absorbed water were numerically additive. As seen in Fig. 10, the swelling of neat resin can be roughly divided into two regions. Region I is from zero volume change to about 2.2% volume change, which corresponds to the initial absorption stage (Fig. 5). The swelling of the resin is far less than the volume of water absorbed in Region II, where the swelling efficiency is increased to close to 1 at volume change above 2.2%. The swelling efficiency, which is the slope at Regions I and II in Fig. 10, of BMI is determined by linear regression. The results are summarized in Table 3. The slope obtained at 100°C is much lower than that obtained at 70°C in region I. The smaller slope corresponds to a lower swelling. The lower swelling indicates less bound water in the system. This finding is consistent with Eq. (5). Addition of more heat will cause the reaction to move in the opposite direction. This is also consistent with higher β at 100°C than at 70°C. In region II, the swelling efficiency is higher at both temperatures, and the difference in slope is smaller, but both are less than 1. This further indicates that the non-Fickian behavior is due to the increased amount of bound water.

4. Discussion

The hydrogen bonds formed during the absorption process are shown in the FTIR spectra (Fig. 8), which are collected on the sample surfaces. Intuitively speaking, the surface should first reach saturation or an equilibrium state with the environment in a short period of time. However, it is clear that the time required for the surface as well as the bulk material to reach saturation is quite long because the process of forming hydrogen bonding is slow. Thus, the slow saturation process in the resin is the main cause of the non-Fickian behavior observed in both BMIs.

Table 3
Linear regression slopes of the swelling experiments

Specimen	Region I		Region II	
	70°C	100°C	70°C	100°C
H-BMI	0.48	0.30	0.77	0.73

Network structure has a great effect on the moisture absorption behavior of BMIs as shown in Fig. 5. The network structure of BMIs is determined by curing schedule (Fig. 1). As the postcuring temperature increases, T_g increases. It is evident that H-BMI is more completely cured than L-BMI (Fig. 1). A system that has higher crosslinking density, which contains more free volume, will have higher diffusivity and M_∞. Plasticization is less significant in H-BMI during hygrothermal conditioning due to its high crosslink density (Fig. 3).

The influence of network structure becomes more obvious if the comparison is made between different temperatures within the same system (Tables 1 and 2). Diffusivity is higher at 100°C than at 70°C for both BMIs. Such behavior is expected and requires no further discussion. As discussed earlier, it is more reasonable to compare M_∞, instead of M_f, values in both BMIs since M_∞ accounts for the whole diffusion process. For both BMIs, M_∞ decreases as the temperatures increase. M_∞ decreases more in L-BMI. This suggests that the mechanism responsible for the change in M_∞ is strongly related to network structure. Soles et al. [14] proposed that the equilibrium moisture uptake is determined by two competing factors: a) dynamic free volume, $V_d(T)$, and b) heat (see Eq. (5)). As the temperature increases, an increase in dynamic free volume $V_d(T)$ will cause an increase in weight gain, while the added heat causes a decrease in weight gain according to Eq. (5). BMI has a rigid network structure because of its aromatic structure. It is less likely that the increase in $V_d(T)$ at 100°C contributes to an increase in weight gain for H-BMI which is close to be fully cured. As temperature increases, the added heat pushes equilibrium towards a lower saturation level (Eq. (5)). This results in a lower M_∞ in H-BMI at higher temperatures. In L-BMI, molecular relaxation should be considered as a third factor beside the two factors proposed by Soles et al. [14]. Since L-BMI is less cured, it relaxes more easily at high temperatures. Molecular relaxation results in smaller free volume, and M_∞ decreases more in L-BMI than in H-BMI at 100°C.

According to Eq. (3), the amount of bound water is determined by the polarity of the system and the amount of unbound water is determined by the available free volume in the system. The two BMIs have similar polarities. Although the availability of polar groups may not be the

same, the difference in M_∞ for the two BMIs mainly comes from the amount of unbound water. Figs. 8 and 10 clearly show that the amount of hydrogen-bonded water is lower at 100°C, which means that water has a higher probability of becoming unbound at higher temperatures. Figs. 8 and 10 also show that water becomes bound and unbound at the beginning of the absorption process. Some free volume is not occupied due to this hydrogen bonding. At a later stage of absorption (Region II in Fig. 10), the swelling efficiency is still less than 1. This suggests that the majority of absorbed water is bound, while some additional water enters free volume, causing no swelling. At lower temperatures, water occupies less free volume due to a higher probability of hydrogen bonding. With an increase in temperature, water activity increases. This allows water to move more freely and occupy more free volume. On the other hand, less water becomes bound due to the added heat. If the system is not fully cured, molecular relaxation will reduce the amount of available free volume, thus further reducing the total water uptake.

The FTIR and swelling experiment results are consistent with the hypothesis of the Langmuir model, i.e. water has a specific probability of interacting with the matrix. This results in a non-Fickian diffusion at longer times. Interestingly, although water can form hydrogen bonds at the beginning of the diffusion process, the Fickian model is still capable of describing the short-term material behavior.

In this study, the Langmuir model can describe the whole diffusion process well since it is based on the nature of the diffusion process in BMI. Unbound water dominates in the early stage and bound water dominates in the later stage of diffusion process. One should realize that the Langmuir model is not perfect for a system with polar groups. Some questions still remain to be answered. According to this model, the probabilities of bound and unbound water do not change during the whole diffusion process. If the system is fully cured and rigid and no chemical reaction is involved, this assumption maybe reasonable. However, if the molecular structure relaxation process can be accelerated by the absorbed water, the free volume of the system will decrease more quickly. Hence, the probabilities of forming the two types of water will also change. The relaxed structure may bring about more accessible polar groups, increasing the amount of bound water or making the material more packed. This leads to a decrease in the amount of unbound water. Under different RH or water activity, the probabilities of bound and unbound water should be different. Carter and Kibler used the same β and γ for all RHs. The present study shows that the probability parameters β and γ change with water activity. Carter and Kibler also suggested that unbound water becomes uniformly distributed long before the bound water, while the swelling experiment results show that the unbound water is diffusing into unoccupied free volume at a later stage of diffusion, as well. Although some modifications may be needed, the Langmuir model appears to be sufficient to describe the diffusion process in BMI resin.

5. Conclusion

It is proposed that the non-Fickian diffusion behavior observed in BMI is due to the hydrogen bonding between water and the matrix. The Langmuir model can be employed to describe this non-Fickian behavior. It takes a long time for equilibrium to be established between bound and unbound water. At the initial stage of absorption, more water that occupies free volume becomes unbound. At the same time, less water can form hydrogen bonds with the polymer to become bound. At a later stage of absorption, the majority of absorbed water is bound, but unbound water can still diffuse into unoccupied free volume. Network structure determined by different curing schedules has an effect on the diffusion behavior of BMI. The less cured system is easier to plasticize by absorbed moisture and relaxes more easily.

Acknowledgements

The authors would like to thank Dow-UT for assisting in the fabrication of composite panels. The funding by the Air Force Office of Scientific Research (Grant No. F49620-98-1-0149) is greatly appreciated.

References

[1] Sillion B. In: Allen G, Bevington JC, editors. Comprehensive polymer science, vol. 5. Oxford: Pergamon Press, 1989.
[2] Chattha MS, Dickie RA. J Appl Polym Sci 1990;40:411.
[3] Stenzenberger HD. In: Kinloch AJ, editor. Structural adhesives: developments in resins and primers. Amsterdam: Elsevier, 1986.
[4] Takekoshi T. Adv Polym Sci 1990;94:1.
[5] Stenzenberger HD, Romer W, Hergenrother PM, Jensen B, Breitigam W. SAMPE J 1990;26:75.
[6] Wei G, Sue H-J. J Appl Polym Sci 1999;74:2539.
[7] Li Y, Tang X, Miranda J, Sue H-J, Whitcomb J, Bradley W. 57th Annu Tech Conf — Soc Plast Engng 1999;3:3423.
[8] Cinquin J, Abjean P. In: 38th International SAMPE Symp Exhib, 1993 May 10–13. p. 1539.
[9] Biney PO, Zhong Y, Zhou J. Int SAMPE Symp Exhib 1998;43:120.
[10] Wilenski M. The improvement of the hygrothermal and mechanical properties of bismaleimide and K3B/IM7 carbon fiber composites through a systematic study of the interphase. PhD Thesis. Michigan: Michigan State University; 1997.
[11] Bao L, Yee AF. Moisture transport and damage initiation in advanced composites. AFOSR Report, September 1999.
[12] Shirrell CD, Halpin J. Composite materials: testing and design (4th conference). ASTM STP 617. American Society for Testing and Materials, 1977. p. 514.
[13] Lee MC, Peppas NA. Prog Polym Sci 1993;18:947.
[14] Soles CL, Chang FT, Bolan BA, Hristov HA, Gidley DW, Yee AF. J Polym Sci, Part B: Polym Phys 1998;36:3035.
[15] Bellenger V, Verdu J, Morel E. J Mater Sci 1989;24:63.
[16] Apicella A, Tessieri R, Cataldis CD. J Membr Sci 1984;18:211.
[17] Adamson MJ. J Mater Sci 1985;15:1736.
[18] Cater HG, Kibler KG. J Compos Mater 1978;12:118.
[19] Barrer RM, Barrie JA, Slater J. J Polym Sci 1958;27:177.
[20] Vieth WR, Sladek KJ. J Colloid 1965;20:1014.
[21] Paul DR, Bunsenges B. Phys Chem 1979;83:294.

[22] Paul DR, Koros WJ. J Polym Sci, Polym Phys Ed 1976;14:675.
[23] Koros WJ, Paul DR, Rocha AA. J Polym Sci, Polym Phys Ed 1976; 14:687.
[24] Petropoulos JH. J Polym Phys A 1970;2(8):1797.
[25] Auze GR, Stern SA. J Membr Sci 1982;12:51.
[26] Mauze GR, Stern SA. J Membr Sci 1984;18:99.
[27] Bonniau P, Bunsell AR. In: Springer GS, editor. Environmental effects of composite materials, vol. 1. Lancaster: Technomic Publishing Company, 1984. p. 209.
[28] Lee MC, Peppas NA. J Appl Polym Sci 1993;47:1349.
[29] Perreux D, Suri C. Comp Sci Technol 1997;57:1403.
[30] Bao L, Yee AF. Personal Communication, September 1999.
[31] Crank J, Park GS, editors. Diffusion in polymers. London: Academic Press, 1968.
[32] Cohen MH, Turnbull DJ. J Chem Phys 1959;31:1164.
[33] King JJ, Chaudhari M. In: 29th National SAMPE Symposium, April 1984. p. 392.
[34] Morgan RJ, Shin EE, Rosenberg B, Jurek A. Polymer 1997;38(3):639.
[35] Phelan JC, Sung CSP. Macromolecules 1997;30:6845.
[36] Yuan Q, Huang F, Jiao Y. J Appl Polym Sci 1996;62:459.
[37] Mijovic J, Andjelic S. Macromolecules 1996;29:239.
[38] Silverstein RM, Webster FX. Spectrometric identification of organic compounds, 6th ed. New York: Wiley, 1997. p. 75.
[39] Sammon C, Mura C. J Phys Chem 1998;102:3402.
[40] Antoon MK, Koenig JL, Serafini T. J Polym Sci, Polym Phys Ed 1981;19:1567.
[41] Deanin RD. Polymer structure, properties and application. Massachusetts: Cahners Books, Division of Cahners Publishing Company, 1972.
[42] Kwei TK. J Appl Polym Sci 1966;10:1647.